Stem Cell Reports, Volume *14*

Supplemental Information

Divergent Effects of *Dnmt3a* and *Tet2* Mutations on Hematopoietic Progenitor Cell Fitness

Elizabeth L. Ostrander, Ashley C. Kramer, Cates Mallaney, Hamza Celik, Won Kyun Koh, Jake Fairchild, Emily Haussler, Christine R.C. Zhang, and Grant A. Challen

Supplemental Experimental Procedures

Mice and transplantation

The Institutional Animal Care and Use Committee at Washington University approved all animal procedures. All mice were C57Bl/6 background. *Dnmt3a*$^{fl/fl}$ (Kaneda et al., 2004) and *Tet2*$^{fl/fl}$ (Moran-Crusio et al., 2011) mice were crossed to *Flt3*^{ITD} (Lee et al., 2007), *Vav-Cre* (Georgiades et al., 2002) and *Mx1-Cre* (Kuhn et al., 1995) strains. To induce *Mx1-Cre*, six doses (300ug) of polyinosinic:polycytidylic acid (pI:pC; Sigma #p1530) were administered every 48-hours via intraperitoneal injection to eight-week old mice. Mice were allowed to recover for six-weeks after the last pI:pC injection prior to sacrifice for donor HSC purification (total age of donor mice = four-months). Equal numbers of male and female mice were pooled for HSC purification for transplantation. Bone marrow transplant recipient mice (C57Bl/6 CD45.1, The Jackson Laboratory strain #002014), received a split dose of lethal irradiation (10.5 Gy) ~4 hours apart. Cells were transplanted via retro-orbital injection. For HSC (CD45.2$^+$ Lineage$^-$ c-Kit$^+$ Sca-1$^+$ CD48$^-$ CD150$^+$) and MPP1 (CD45.2$^+$ Lineage$^-$ c-Kit$^+$ Sca-1$^+$ CD48$^-$ CD150$^-$) transplants, 200 donor cells were purified by flow cytometry and transplanted into lethally irradiated CD45.1 recipients with 2.5x10^5 wild-type CD45.1 WBM support. MPP3 (CD45.2$^+$ Lineage$^-$ c-Kit$^+$ Sca-1$^+$ CD48$^+$ CD150$^-$) transplant recipients received 250 purified cells in addition to the WBM support. For secondary transplants, donor-derived HSCs were purified from primary recipients and transplanted (200 per mouse) with 2.5x10^5 fresh CD45.1 WBM support into secondary recipients. Tertiary transplants were performed in a similar manner. Genotyping primers are presented in the table below;

Gene	Primer Sequence
Vav-CRE Forward	AGATGCCAGGACATCAGGAACCTG
Vav-CRE Reverse	ATCAGCCACACCAGACACAGAGATC
Mx-1 CRE Forward	CTGGGGATTGCTTATAACACCC
Mx-1 CRE Reverse	TCATCAGCTACACCAGAGACGG
Tet2 Forward	AAGAATTGCTACAGGCCTGC
Tet2 Reverse	TTCTTTAGCCCTTGCTGAGC
Dnmt3a Forward	ATCACATTACCTTTGTCCTCCCAGATCCAG
Dnmt3a Reverse	AGGCTGTCTGCATCGGACAGTGAGTGGTG

Flow Cytometry

Cells were stained in Hanks Balanced Salt Solution (HBSS, Corning #21021CV) containing Pen/Strep (100Units/mL, Fisher Scientific #MT30002CI), HEPES (10μM, Life Technologies #15630080) and Serum Plus II (2%, Sigma #14009C) at a density of 1.0x10^8/mL. Staining was performed for >20 minutes at 4^{o}C with the following anti-mouse antibodies (1:100 dilutions, all from BioLegend unless stated otherwise): CD45.1 (clone

A20, #110706), CD45.2 (clone 104, #84208), B220 (clone A20, #103212), Gr-1 (clone RB6-8C5, #108416), Mac-1 (clone M1/70, #101216), CD3e (clone 145-2C11, #100312), Ter119 (clone TER-119, #116223), NK1.1 (clone PK136, eBiosciences #13-5941-85), CD48 (clone HM48-1, #103424), CD150 (clone TC15-12F12.2, #115904), c-Kit (clone 2B8, #84158), Sca-1 (clone E13-161.7, #122512), CD11c (clone N418, eBiosciences #13-0114-82), CD5 (clone 53-7.3, #100622), CD19 (clone 6D5, #115520), F4/80 (clone BM8, #123133), Ly6C (clone HK1.4, #128005), Ly6G (clone 1A8, #127627). Negative controls used to set gates were established using fluorescence minus one (FMO) tubes for a parameter of interest, or isotype staining controls.

WBM was isolated from tibias, femurs, and iliac crests and combined for calculating total WBM from each mouse. Hematopoietic progenitor cells were purified via flow cytometry from enriched WBM using anti-mouse CD117-conjugated microbeads (Miltenyi Biotec #130-091-224). WBM was incubated on ice with microbeads for 30 minutes and enriched using the AutoMACS Pro Separator (Miltenyi Biotec #130-092-545). Post-enrichment, samples were stained with antibodies for cell sorting. Peripheral blood from transplant recipients was analyzed for test (CD45.2) and competitor (CD45.1) contributions to hematopoietic lineages by FACS using the two CD45 isoform antibodies as well as myeloid (Gr-1+ and Mac-1+), B-cell (B220+) and T-cell (CD3e+) antibodies.

Methocult Colony Forming Assays

Colony forming assays were performed by plating 100 HSCs, MPP1, and MPP3, or $1.0x10^4$ WBM cells into a 6-well plate with 2mL of methocellulose-based medium (MethoCult M3434, Stemcell Technologies #03434). Colonies were scored on day nine for the first plating. Serial colony formation potential was determined by passaging 10,000 cells isolated from the previous plating into new 6-well plates with 2mL of Methocult M3434. Colonies were scored on day 7 for serial passages.

Differentiation Assay

Myeloid differentiation potential was assessed by plating 225 HSCs, MPP1, or MPP3 onto OP9 stromal cells in MEM-Alpha (Gibco # LS12571063) supplemented with Pen-Strep (100 units/mL), mSCF (50 ng/mL), mFlt3L (10 ng/mL), and mIL-3 (10 ng/mL), mGM-CSF (10 ng/mL), mM-CSF (10 ng/mL), and mG-CSF (10 ng/mL). Cells were analyzed via flow cytometry for immunophenotyping: dendritic cells (NK1.1-, CD5-, CD19-, Mac-1+, CD11c+), neutrophils (NK1.1-, CD5-, CD19-, Mac-1+, CD11c-, Ly6G+, Ly6C+), monocytes (NK1.1-, CD5-, CD19-, Mac-1+, CD11c-, Ly6G-, Ly6C+, F4/80-), macrophages (NK1.1-, CD5-, CD19-, Mac-1+, CD11c-, Ly6G-, Ly6C+, F4/80+).

RNA-SEQ data, quality control and analysis

HSCs and MPP3 were purified from four biological replicates (pooled WBM from two male and two female mice). A NucleoSpin RNA XS kit (Macherey-Nagel #740902.250) was used to isolate RNA. Library preparation,

sequencing, and alignment was performed by the Genome Technology Access Center (Washington University). The SMARTer Ultra Low RNA kit (Clontech) was used to prepare the libraries from 3-5ng of total RNA. Sequencing was performed with an Illumina HiSeq-3000. Reads were aligned with STAR (Dobin et al., 2013) version 2.5.4b with Gencode release M20 (GRCm38.p6) genome assembly. Unambiguous read counts were calculated by HTSEQ-count (Anders et al., 2015) version 0.6.0 with mode "intersection-strict." Expression data were imported into Noiseq v2.28.0 (Tarazona et al., 2015) for differential gene expression analysis with TMM normalization and batch correction. Gene set enrichment analysis was performed with fGSEA v1.10.0. Primary RNA-SEQ data is available under GEO accession number GSE139911.

ATAC-seq

Open chromatin was profiled using a modified Omni-ATAC method (Corces et al., 2017). Briefly, 10,000 HSCs, MPP1, and MPP3 were sorted by flow cytometry into 500 µL of PBS + 0.2% BSA. Cells were pelleted and resuspended in 50 µL of ATAC-RSB buffer with 0.1% NP40, 0.1% Tween-20, and 0.01% digitonin and incubated on ice for three minutes. Samples were washed with ATAC-RSB buffer with 0.1% Tween-20 and nuclei were pelleted and resuspended in transposition reaction mixture with transposase (Nextera) for 30 minutes at 37^{o}C and 1000 RPM shaking. DNA was purified using Zymo DNA Clean and Concentrator-5 Kit (Zymo #D4014). Libraries were amplified using NEBnext (New England Biolabs) with custom Nextera primers. Cycle number was determined with qPCR as previously described. Libraries were purified with Ampure XP beads. Libraries were sequenced with an Illumina HiSeq-3000 (PE2X150). ATAC-seq reads were aligned to mm10 with BWA mem v0.7.17. Duplicates were removed with Picard tools MarkDuplicates v2.0.1 and the resulting bams were processed with snakePipes v1.3.1 (Bhardwaj et al., 2019) ATAC-seq pipeline. A consensus peak set was derived by comparing narrrowPeak files for each replicate and keeping a peak region if present in at least two replicates. Differential chromatin accessibility was assessed by downsampling the filtered bam outputs from snakePipes to the smallest represented library size and counting the reads that fell into the consensus peaks using Rsubread v1.34.7 (Liao et al., 2019). The resulting count matrix was analyzed via EdgeR v3.26.8 (Robinson et al., 2010) for differential read counts keeping the starting library size throughout the analysis. Peaks were annotated with genomic features using csaw v1.18.0. Peaks were also intersected with enhancers (Aranda-Orgilles et al., 2016) using bedtools v2.25.0. Bigwig tracks and heatmaps were created through deepTools2 v3.3.1 (Ramirez et al., 2016). Tracks were visualized with IGV v2.7.2. Gene ontology analysis was performed with GREAT v4.0.4 (McLean et al., 2010). Primary ATAC-seq data is available under GEO accession number GSE139911.

Statistics

Student t-test, one-way, and two-way ANOVA's were used for statistical comparisons where appropriate. Kruskal-wallis test was used for non-normal data. Survival curves were analyzed using a Mantel-Cox logrank

test. Significance is indicated using the following convention: *p <0.05, **p <0.01, ***p <0.001, ****p <0.0001. All graphs represent mean ± S.E.M.

Supplemental Figures

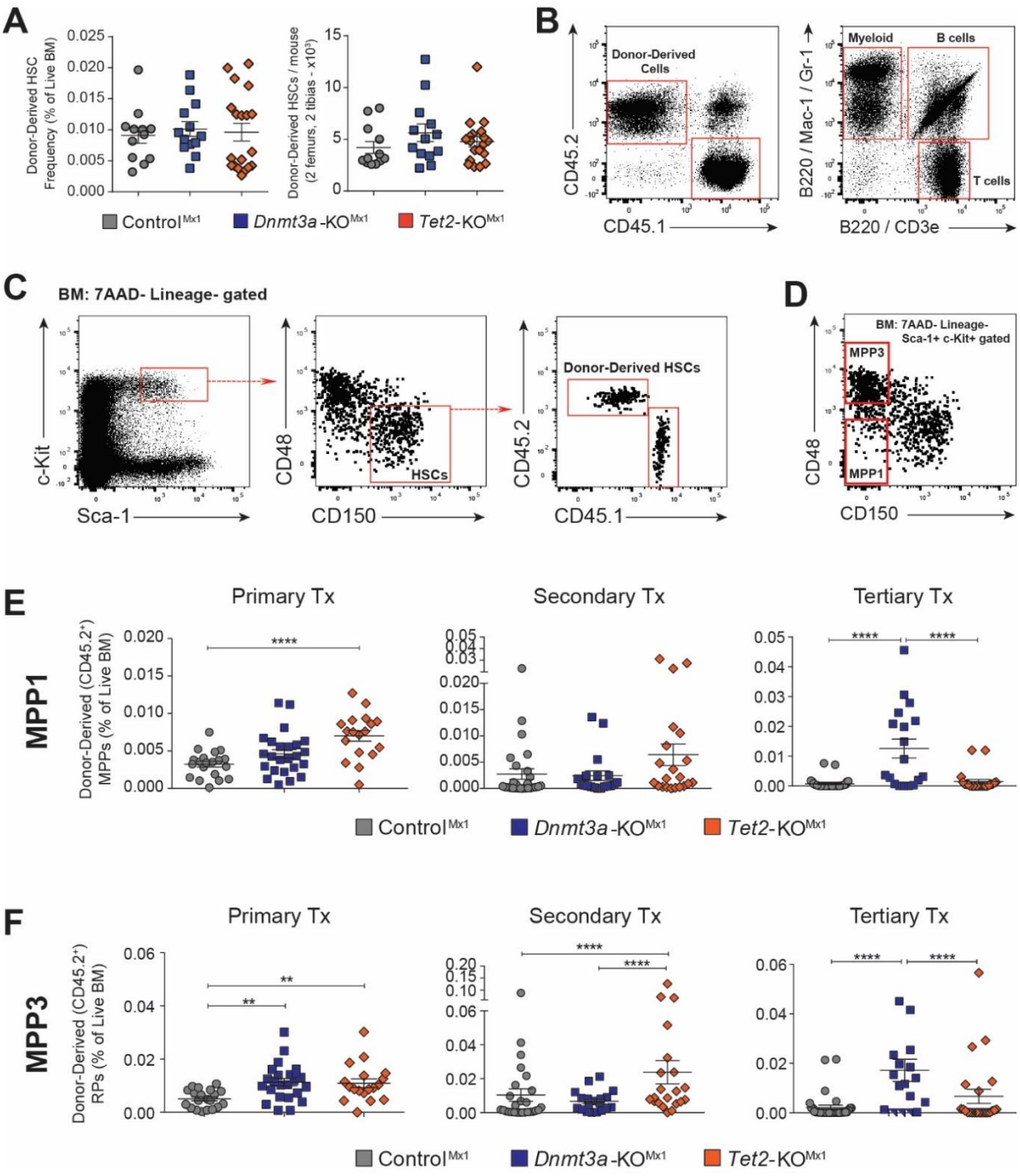

Figure S1: ***Loss of Dnmt3a and Tet2 Enhance Self-Renewal in HSCs to Different Degrees, Related to Figure 1.***

(A) Frequency and absolute numbers of HSCs from adult *Mx1-Cre* mouse strains six-weeks after the last pIpC injection at time of sacrifice for HSC purification for transplantation. (B) Flow cytometry plots of representative gating for peripheral blood analysis. (C) Representative flow cytometry plots of BM from recipient mice defining donor-derived HSCs. (D) Flow cytometry plots of representative gating for MPP1 and MPP3 populations. Frequency of donor-derived (E) MPP1 and (F) MPP3 from transplantation of Control^{Mx1} (CNT), *Dnmt3a*-KO^{Mx1} (3aKO), and *Tet2*-KO^{Mx1} (T2KO) HSCs at 18-weeks following primary (CNT *n*=28; 3aKO *n*=24; T2KO *n*=22), secondary (CNT *n*=27; 3aKO *n*=19; T2KO *n*=21), and tertiary (CNT *n*=33; 3aKO *n*=23; T2KO *n*=19) transplants. **p* < 0.05, ***p* < 0.01, ****p* < 0.001, *****p* < 0.001. Mean ± S.E.M. values are shown.

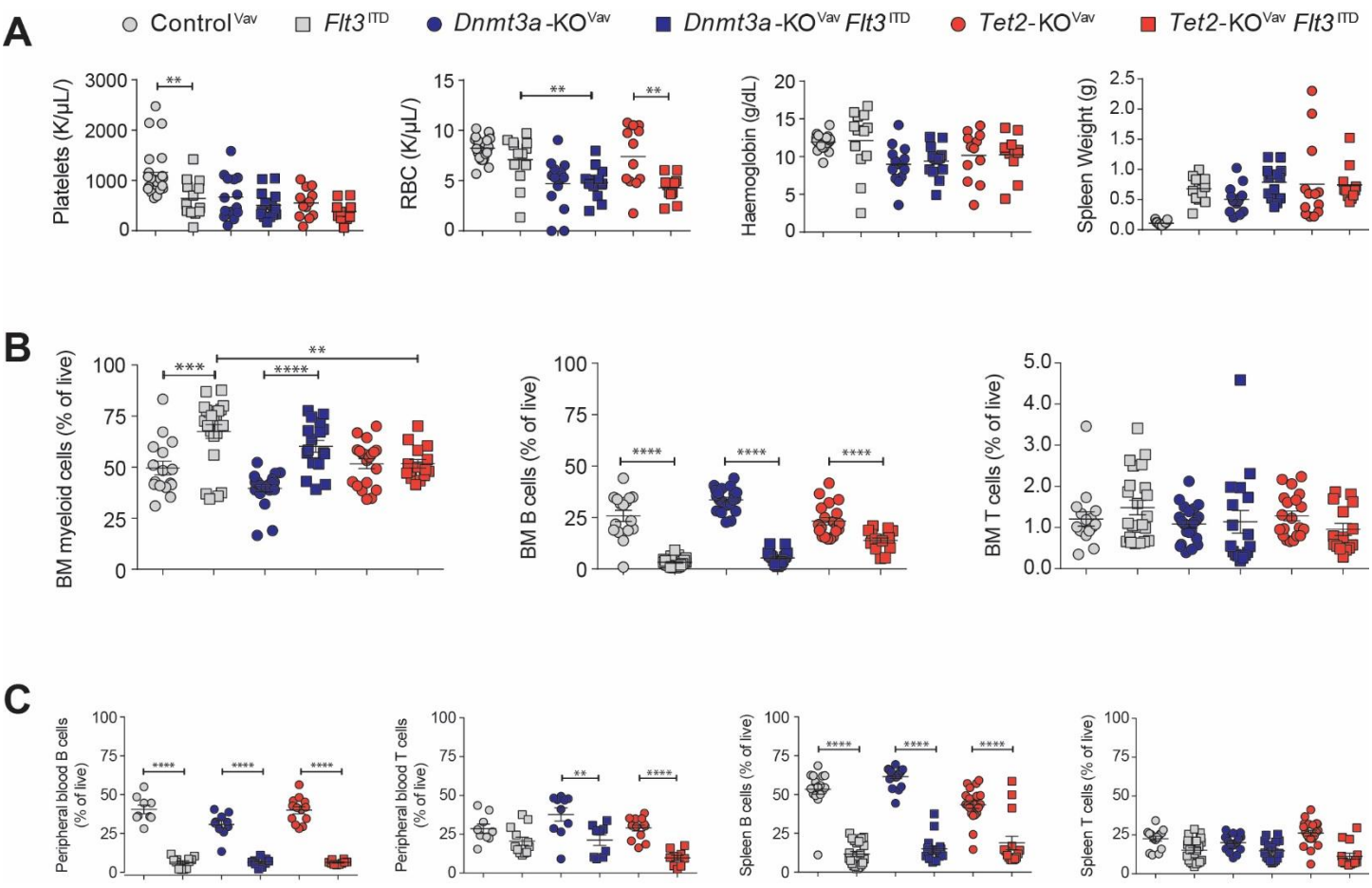

Figure S2: ***Tet2 and Dnmt3a loss-of-function divergently influence hematopoietic progenitor cells, Related to Figure 2.***

(A) Platelet counts, RBC, hemoglobin, and spleen weights of moribund mice. (B) BM myeloid, B-cell, and T-cell distribution of 8-week old mice from indicated genotypes. (C) Proportion of B-cells and T-cells in peripheral blood and spleens of mice from eight-week old Control^{Vav} (*n*=18), *Flt3*^{ITD} (*n*=14), *Dnmt3a*-KO^{Vav} (*n*=18), *Dnmt3a*-KO^{Vav}*Flt3*^{ITD} (*n*=10), *Tet2*-KO^{Vav} (*n*=15), and *Tet2*-KO^{Vav}*Flt3*^{ITD} (*n*=9) mice. ***p* < 0.01, ****p* < 0.001, *****p* < 0.001. Mean ± S.E.M. values are shown.

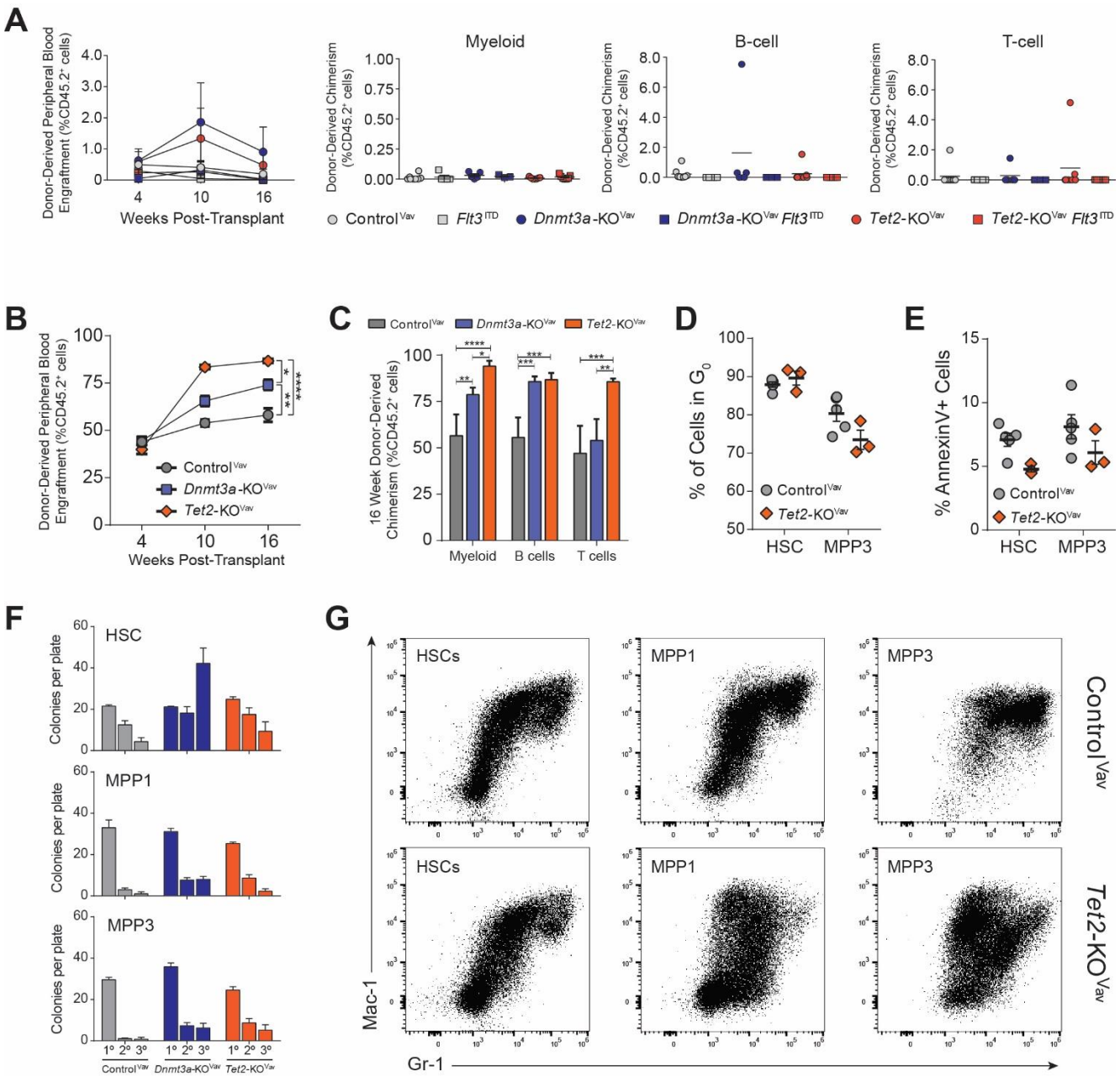

Figure S3: ***Tet2 Mutation Does Not Impart Ectopic Self-Renewal to Hematopoietic Progenitors But Skews Myeloid Differentiation of Committed Progenitor Cells, Related to Figure 3.***

(A) Donor-derived peripheral blood cells and 16-week lineage chimerism in recipients of 250 MPP3 from Control^{Vav} (n=8), *Flt3*^{ITD} (n=5), *Dnmt3a*-KO^{Vav} (n=5), *Tet2*-KO^{Vav} (n=7), *Dnmt3a*-KO^{Vav}*Flt3*^{ITD} (n=3), or *Tet2*-KO^{Vav}*Flt3*^{ITD} (n=7) mice. (B) Donor-derived peripheral blood cells and (C) 16-week lineage chimerism in recipients of 5.0x10^5 BM from Control^{Vav} (n=5), *Dnmt3a*-KO^{Vav} (n=5) and *Tet2*-KO^{Vav} (n=4) mice competed against 5.0x10^5 CD45.1 BM. (D) Percentage of quiescent (G_0) HSCs and MPP3 in Control^{Vav} (n=5) and *Tet2*-KO^{Vav} (n=3) mice by Ki67 / DAPI flow cytometry. (E) Percentage of apoptotic HSCs and MPP3 in Control^{Vav} (n=5) and *Tet2*-KO^{Vav} (n=3) mice by AnnexinV flow cytometry. (F) Colony counts from serial replating assays (n=6-10 per genotype). (G) Representative flow cytometry plots of *in vitro* differentiated cells from Control^{Vav} and *Tet2*-KO^{Vav} mice. *p < 0.05, **p < 0.01, ***p < 0.001, ****p < 0.001. Mean ± S.E.M. values are shown.

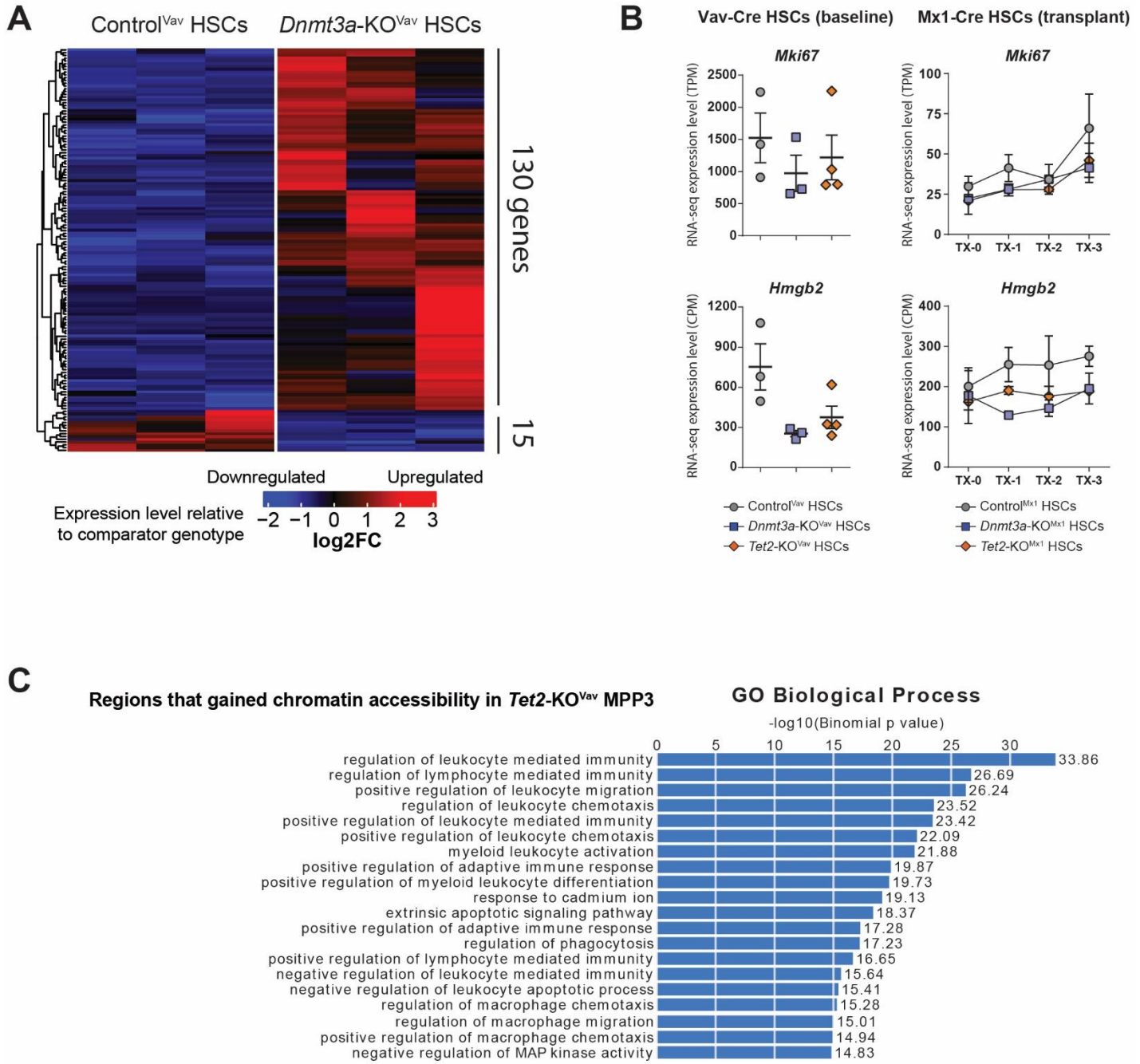

Figure S4: ***Dnmt3a and Tet2 Loss of Function Alter Hematopoietic Progenitor Function Through Distinct Molecular Mechanisms, Related to Figure 4.***

(A) Heatmap displaying differentially expressed genes (p<0.05, fold-change > 1 or < -1) between Control^{Vav} and *Dnmt3a*-KO^{Vav} HSCs. (B) Transcriptional profile of genes commonly downregulated in *Dnmt3a*-KO^{Vav} and *Tet2*-KO^{Vav} HSCs across serial transplant (TX) of *Mx1-Cre* HSCs. (C) Gene ontology analysis of the genomic regions that gained chromatin accessibility in *Tet2*-KO^{Vav} MPP3 using GREAT. Enrichment of the top 20 GO biological processes are displayed.

Supplemental Tables

Table S1: Gene expression in HSCs across serial transplantation. Related to Figure 4.

Normalized RNA-seq gene expression values (counts per million = cpm) of Control^{Mx1}, *Dnmt3a*-KO^{Mx1}, and *Tet2*-KO^{Mx1} HSCs across serial competitive transplantation.

Table S2: Gene expression in HSCs and MPP3s. Related to Figure 4.

Normalized RNA-seq gene expression values (transcripts per million = tpm) of Control^{Vav}, *Dnmt3a*-KO^{Vav}, and *Tet2*-KO^{Vav} HSCs and MPP3s.

Table S3: Open chromatin profiling in HSCs, MPP1s and MPP3s. Related to Figure 4.

Differential regions of open chromatin from ATAC-seq analysis of Control^{Vav}, *Dnmt3a*-KO^{Vav}, and *Tet2*-KO^{Vav} HSCs, MPP1s and MPP3s.

Supplemental References

Anders, S., Pyl, P. T., and Huber, W. (2015). HTSeq--a Python framework to work with high-throughput sequencing data. Bioinformatics *31*, 166-169.

Aranda-Orgilles, B., Saldana-Meyer, R., Wang, E., Trompouki, E., Fassl, A., Lau, S., Mullenders, J., Rocha, P. P., Raviram, R., Guillamot, M.*, et al.* (2016). MED12 Regulates HSC-Specific Enhancers Independently of Mediator Kinase Activity to Control Hematopoiesis. Cell Stem Cell *19*, 784-799.

Bhardwaj, V., Heyne, S., Sikora, K., Rabbani, L., Rauer, M., Kilpert, F., Richter, A. S., Ryan, D. P., and Manke, T. (2019). snakePipes: facilitating flexible, scalable and integrative epigenomic analysis. Bioinformatics *35*, 4757-4759.

Corces, M. R., Trevino, A. E., Hamilton, E. G., Greenside, P. G., Sinnott-Armstrong, N. A., Vesuna, S., Satpathy, A. T., Rubin, A. J., Montine, K. S., Wu, B.*, et al.* (2017). An improved ATAC-seq protocol reduces background and enables interrogation of frozen tissues. Nat Methods *14*, 959-962.

Dobin, A., Davis, C. A., Schlesinger, F., Drenkow, J., Zaleski, C., Jha, S., Batut, P., Chaisson, M., and Gingeras, T. R. (2013). STAR: ultrafast universal RNA-seq aligner. Bioinformatics *29*, 15-21.

Georgiades, P., Ogilvy, S., Duval, H., Licence, D. R., Charnock-Jones, D. S., Smith, S. K., and Print, C. G. (2002). VavCre transgenic mice: a tool for mutagenesis in hematopoietic and endothelial lineages. Genesis *34*, 251-256.

Kaneda, M., Okano, M., Hata, K., Sado, T., Tsujimoto, N., Li, E., and Sasaki, H. (2004). Essential role for de novo DNA methyltransferase Dnmt3a in paternal and maternal imprinting. Nature *429*, 900-903.

Kuhn, R., Schwenk, F., Aguet, M., and Rajewsky, K. (1995). Inducible Gene Targeting in Mice. Science *269*, 1427-1429.

Lee, B. H., Tothova, Z., Levine, R. L., Anderson, K., Buza-Vidas, N., Cullen, D. E., McDowell, E. P., Adelsperger, J., Frohling, S., Huntly, B. J.*, et al.* (2007). FLT3 mutations confer enhanced proliferation and survival properties to multipotent progenitors in a murine model of chronic myelomonocytic leukemia. Cancer Cell *12*, 367-380.

Liao, Y., Smyth, G. K., and Shi, W. (2019). The R package Rsubread is easier, faster, cheaper and better for alignment and quantification of RNA sequencing reads. Nucleic Acids Res *47*, e47.

McLean, C. Y., Bristor, D., Hiller, M., Clarke, S. L., Schaar, B. T., Lowe, C. B., Wenger, A. M., and Bejerano, G. (2010). GREAT improves functional interpretation of cis-regulatory regions. Nat Biotechnol *28*, 495-501.

Moran-Crusio, K., Reavie, L., Shih, A., Abdel-Wahab, O., Ndiaye-Lobry, D., Lobry, C., Figueroa, M. E., Vasanthakumar, A., Patel, J., Zhao, X.*, et al.* (2011). Tet2 loss leads to increased hematopoietic stem cell self-renewal and myeloid transformation. Cancer Cell *20*, 11-24.

Ramirez, F., Ryan, D. P., Gruning, B., Bhardwaj, V., Kilpert, F., Richter, A. S., Heyne, S., Dundar, F., and Manke, T. (2016). deepTools2: a next generation web server for deep-sequencing data analysis. Nucleic Acids Res *44*, W160-165.

Robinson, M. D., McCarthy, D. J., and Smyth, G. K. (2010). edgeR: a Bioconductor package for differential expression analysis of digital gene expression data. Bioinformatics *26*, 139-140.

Tarazona, S., Furio-Tari, P., Turra, D., Pietro, A. D., Nueda, M. J., Ferrer, A., and Conesa, A. (2015). Data quality aware analysis of differential expression in RNA-seq with NOISeq R/Bioc package. Nucleic Acids Res *43*, e140.